Journal of Materials Chemistry B

Accepted Manuscript

ROYAL SOCIETY OF CHEMISTRY

www.rsc.org/materialsB

Cite this: DOI: 10.1039/c0xx00000x

www.rsc.org/xxxxxx

ARTICLE TYPE

Organoamine-assisted biomimetic synthesis of faceted hexagonal hydroxyapatite nanotubes with prominent stimulation activity for osteoblast proliferation

Xiangke Guo, Liang Yu, Lanhua Chen, Heyun Zhang, Luming Peng, Xuefeng Guo,* Weiping Ding

Received (in XXX, XXX) Xth XXXXXXXXX 20XX, Accepted Xth XXXXXXXXX 20XX
DOI: 10.1039/b000000x

Uniform single-crystalline hydroxyapatite nanotubes with hexagonal facets have been synthesized via a distinctive organoamines-assisted biomimetic route. These novel HA nanotubes exhibit exceptional performance in stimulating osteoblast proliferation, which endows them intriguing potential for bone repair.

Hydroxyapatite($Ca_{10}(PO_4)_6(OH)_2$, denoted as HA in the context), is of considerable interest for their potential applications as biomaterial, adsorbent, ion exchanger, catalyst or catalyst support due to their special ion-exchange ability, adsorption capacity, and acid-base properties.[1] Particularly, HA as the main mineral constituent of animal and human bone, has attracted extensive attention in bone tissue engineering because of its high biocompatibility and osteoconductivity.[2] The hierarchical structure and morphology of HA are important, which may affect its performance significantly.[3] Hence there has been great interest in developing new strategies to fabricate novel morphology and hierarchical structures of HA for out-bound performance, in despite of the considerable difficulties arisen from the complexity of HA crystallization.[4]

The formation of HA in creatures is a very slow biomineralization process accompanying with the crystal phase evolution of calcium phosphates, which is controlled by proteins with acidic amino acid residues ingeniously.[5] Inspired by the biomineralization process, most investigators focused material-design of HA on carboxylate group-rich organic molecules, such as collagen, citrate, and etc., to control the nucleation, growth and morphology of HA crystals since carboxylate group binds effectively to Ca^{2+}.[6] However, the role of amino group, the other important moiety on amino acid, is ignored. Meanwhile, although many methods have been successfully adopted to fabricate HA with various morphology and structure,[7] only a few uncommon approaches were reported to achieve impure HA nanotubes, for example, nanotubular HA composed of nanoparticles formed in porous alumina template,[7c] nanotubular F-containing HA synthesized from CaF_2 precursor,[7d] and HA nanowire/nanotube arrays prepared by a solvothermal synthesis.[7e] Up to date, the synthesis of high-quality impurity-free HA nanotubes still remains a challenge.

Herein, we report a distinctive biomimetic process to fabricate pure HA single crystalline nanotubes just using organoamines as inducer and controller. The obtained HA products are uniform nanotubes with hexagonal face and open tips. Our investigations discover a novel process that how carboxylate group-free organoamine molecules (dodecylamine and hexadecylamine) induce the formation of HA nanotubes through a dual evolution of crystal phase and morphology: from $CaHPO_4•2H_2O$ (DCPD) rectangular plates to $CaHPO_4$ (DCP) nanorods and from $CaHPO_4$ nanorods to $Ca_{10}(PO_4)_6(OH)_2$ nanotubes. And more importantly, these novel single-crystalline nanotubes strikingly present

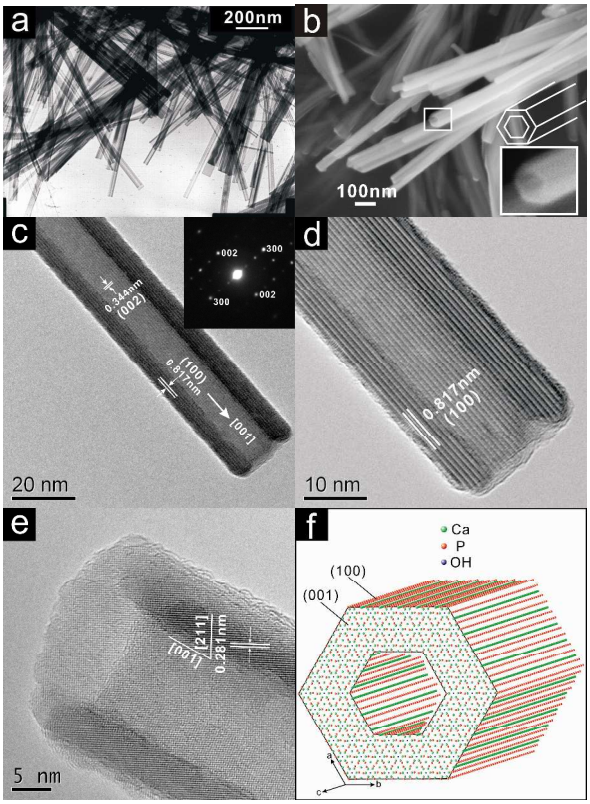

Fig. 1 HA nanotubes obtained after 48 hours of hydrothermal treatment at 393 K. a) TEM; b) SEM; c); d) and e) HRTEM images. The inset of c shows the SAED pattern taken at the nanotube; b) a crystal model of HA nanotube. Only the surface atoms are shown: the points are calcium (green), phosphorus (red) and hydroxyls (deep blue) and the oxygen atoms in phosphate are omitted for clarity.

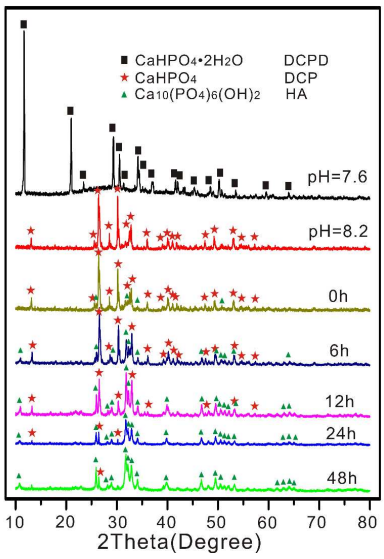

Fig. 2 XRD patterns of the samples obtained at different synthetic stages.

exceptional performance in stimulating osteoblast proliferation, even more effective than natural bone morphogenetic protein-7 (BMP-7).

Typical electron microscopy images of the prepared HA nanotubes are shown in Fig. 1. The TEM image (Fig. 1a) clearly shows the hollow one-dimensional structures of the products with open ends. These nanotubes are several micrometers in length with inner and outer diameters of ca. 8~50 nm and 20~80 nm, respectively. SEM image (Fig. 1b) and HRTEM image of the cross section of a single HA nanotube (see Supplementary Information (SI), Fig. S1) reveal the hexagonal faceted 1D structure of the nanotubes, consistent with the hexagonal structure of HA. Fig. 1c and Fig. 1d depict HRTEM images of an individual nanotube with lattice fringes of planes corresponding to (100) planes parallel to the nanotube axis, implying that the axis is along the [001] direction of HA. This is a frequent growth characteristic for onedimensional materials with hexagonal structure. The inset of Fig. 1c is a selected area electron diffraction pattern (SAED) taken at the single nanotube, indicating the nanotube is single crystalline and the axial direction is [001] of HA. The HRTEM image in Fig. 1e taken at the open tip of another individual nanotube also indicates the tube is HA single crystal. The lattice fringes of planes with a d-spacing of 2.81 Å correspond to (211) planes of HA. Based on these structural data, a crystal model of HA nanotube is proposed in Fig. 1f, with realistic outer and inner surfaces. In the synthesis, the amino groups of organoamines have interactions with the phosphate groups of HA crystal, which may contribute to the surfacial (100) planes of HA nanotubes with more PO_4^{3-} groups.[8]

The biomimetic process which leads to HA nanotubes formation was carefully monitored to investigate the evolution of the morphologies and crystal phases of calcium phosphate. The synthetic process could be divided into two steps: the slow dropwise addition of the organoamines solution into the mixed solution ($Ca(H_2PO_4)_2$ and $CaCl_2$ in water) and the hydrothermal process. In the first stage, along with the very slow addition of the organoamines, the pH value of the system increased from 4.3 to 9.5 gradually, meanwhile the amino groups reacted with the dihydrogen phosphate ions to result in precipitation (SI, Fig. S2a,). When the pH value was below 8.2, only regular rectangular plates were observed (SI, Fig. S2b). The plates were determined as $CaHPO_4•2H_2O$ (DCPD) (XRD patterns shown in Fig. 2), which is the predominant phase of calcium phosphate precipitated at low pH conditions.[4b] When the pH value increased to 8.2, all the nanoplates disappeared and only nanofibers were observed (SI, Fig. S2c), which occurred in a very narrow pH window. The nanofibers were determined as $CaHPO_4$ (DCP) according to the XRD data (Figure 3).

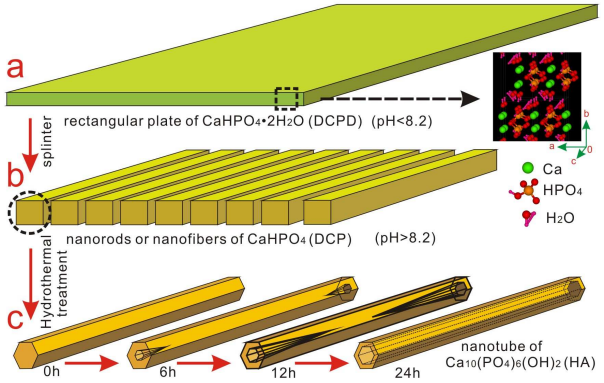

Fig. 3 Schematic show of the formation mechanism of HA nanotubes. a) DCPD plates formed at pH lower than 8.2. The top right inset is the crystal structure of DCPD, of which lattice water molecules are between the calcium phosphate chains along the c direction. b) DCP nanofibers formed by the dehydration and splitting of DCPD plates along c axis at pH value higher than 8.2. c) HA nanotube transformed from DCP nanofibers step by step during the hydrothermal treatment. The hollow structure spread from tips to the middle and then the whole tubular structure formed at the end. The organoamines molecules on the solids are omitted in the figure for clarity.

Fig. S2d-2g (SI) shows the process of morphology transformation of the calcium phosphate during the hydrothermal process. After 6 hours of hydrothermal treatment, the starting DCP fibers (SI, Fig. S2d) were converted to partially hollow fibers (hollow at both ends of the fibers (SI, Fig. S2e)). Meantime, the XRD results of these fibers indicate the appearance of the HA phase (Fig. 2), which is more stable under alkaline conditions.[4b] Since the atomic ratio of Ca : P is 1 : 1 for DCP and 1.67 : 1 for HA, the transformation of DCP to HA must be accompanied by the dissolving of PO_4^{3-} from the DCP nanofibers due to the reaction of CaHPO4 with organoamines, which accounts for the formation of the hollow structures. Since the organoamines adsorbed on the surface (SI, Fig. S2c), the surface layer of the DCP fibers transformed to HA crystal structure firstly and kept the rod shape simultaneously. Prolonged hydrothermal treatment causes further removal of PO_4^{3-} from the inner space of nanofibers which leads to the formation of the nanotubes with open ends (SI, Fig. S2f and S2g). After 24 hours of hydrothermal treatment, the products are almost nanotubes (SI, Fig. S2g). The subsequent hydrothermal treatment (till 48 hours) leads to more regular shape and better crystallization of the nanotubes (Fig. 1a and Fig. 2).

The XRD profiles of the products obtained at different time of hydrothermal treatment are shown in Fig. 2. The crystal phase transformation from DCP to HA during the hydrothermal treatment is very clear, which accords very well with the morphology transformation. After prolonged hydrothermal treatment (48 hours), almost all the diffraction peaks can be well indexed to the hexagonal HA ($Ca_{10}(PO_4)_6(OH)_2$, JCPDS72-1243).

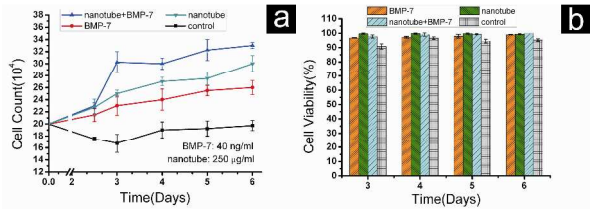

Fig. 4 HA nanotubes boost the cell proliferation. a) The cell proliferation curves of osteoblasts cultured with HA nanotubes and BMP-7. The break parts in the proliferation curves are induction periods of osteoblasts culture. b) The corresponding cell viability histograms. Cell viability is expressed as the percentage of number of viable cells compared to total number of cells. Error bars represent the standard deviation for six

Based on the above systematical studies, the biomimetic process of the formation of the HA nanotubes in presence of organoamines is schematically described as Fig. 3: It is a synergic evolution of outer morphology and inner crystalline phase of inorganic species. Both the organoamine molecules and their very slow addition are pivotal for the formation of HA nanotubes. The extremely slow addition of organoamines mimicking the slow process of biomineralization, allow the regular DCPD plates to form and further transform into nanorod-like intermediate (DCP), otherwise tanglesome precipitate is obtained instead. It is well known that HA phase can be transformed from DCPD phase and DCP phase,[9] and HA nanorods can be obtained from octacalcium phosphate (OCP) plates.[10] Recently, the evolution process from the calcium phosphate precursor sheets to HA nanowires/nanotubes arrays under solvothermal condition has also been reported.[7e] However, to the best of our knowledge, this formation process of HA nanotubes: from DCPD plates to DCP nanorods and future to HA nanotubes, is never discovered before.

It has been shown that an interplay exists between osteoblasts and nanoapatite features.[11] Here we culture the murine osteoblasts with HA nanotubes *in vitro* to investigate the effects of HA nanotubes on cell proliferation and migration, in the absence of osteogenic supplements. The results of the 6-day cell culture in vitro are shown in Fig. 4. From the cell proliferation curves (Fig. 4a), one can see that the nanotubes boost the cell proliferation significantly, i.e., the cellular numbers in the sample with nanotubes (the dose of HA nanotubes is 250 μg/ml) increased 1.5 times (from 20×10^4 to 30×10^4), while those of the control remained largely unchanged. More interestingly, the nanotubes are even more effective in accelerating the cell proliferation than BMP-7 (Fig. 4a), a member of transforming growth factor β (TGF-β) family which are key modulators of cell proliferation, differentiation, and etc. When nanotubes are combined with BMP-7 in the cell culture, a positive synergistic effect is observed (Fig. 4a, blue curve). Moreover, cell viability on cytotoxicity test of the nanotubes is shown in Fig. 4b: the nanotubes are noncytotoxic and even show slightly better effect on the cell viability. The boosting effect on cell proliferation can also be seen clearly using an inverted microscope, as shown in Fig. S3. Interestingly, the cells tend to migrate together and proliferate radially around the aggregation of the nanotubes (inset of Fig. S3b). The HA nanotubes possess special hollow nanostructure and large surface area to adsorb proteins, offering many more binding sites to cell membrane receptors, which might benefit the cell proliferation and migration.[12]

In conclusion, we develop an unprecedented organoamines-assisted biomimetic route to fabricate impurity-free HA nanotubes. Single crystalline HA nanotubes with hexagonal face and open tips were synthesized and a novel formation process of nanotube was discovered. More importantly, the results of cell culture showed that the obtained pure nanotubular HA was highly efficient in encouraging cell proliferation, which endows it great potential for bone repair. Studies on the catalytic performance and selective separation of the novel nanotubes are also under way.

This work was financially supported by the National Basic Research Program (2009CB623504), the National Science Foundation of China (21173119, 21273109, 21303083), the Natural Science Foundation of Jiangsu Province (SBK201340143) and the Specialized Research Fund for the Doctoral Program of Higher Education (20130091120045).

Notes and references

Key Lab of Mesoscopic Chemistry, School of Chemistry and Chemical Engineering, Nanjing University, Nanjing 210093, China. Fax: +86 25 83317761; Tel: +86 25 83686393; E-mail: guoxf@nju.edu.cn.

† Electronic Supplementary Information (ESI) available: Experimental Section, HRTEM, TEM images and inverted microscope images. See DOI: 10.1039/b000000x/

1 (a) L. J. Ji, G. Jell, Y. X. Dong, J. R. Jones and M. M. Stevens, *Chem. Commun.*, 2011, **47**, 9048; (b) M. Brand, S. Rampalli, C. P. Chaturvedi and F. J. Dilworth, *Nat. Protoc.*, 2008, **3**, 398; (c) K. Mori, T. Hara, T. Mizugaki, K. Ebitani and K. Kaneda, *J. Am. Chem. Soc.*, 2004, **126**, 10657; (d) Y. M. Liu, H. Tsunoyama, T. Akitabc and T. Tsukuda, *Chem. Commun.*, 2010, **46**, 550; (e) M. Zahmakıran, Y. Tonbul and S. Özkar, *Chem. Commun.*, 2010, **46**, 4788.

2 (a) S. V. Dorozhkin and M. Epple, *Angew. Chem. Int. Ed.*, 2002, **41**, 3130; (b) R. Z. LeGeros, *Chem. Rev.*, 2008, **108**, 4742; (c) J. M. Anderson, J. L. Patterson, J. B. Vines, A. Javed, S. R. Gilbert and H. W. Jun, *ACS Nano*, 2011, **5**, 9463.

3 (a) A. Tampieri, S. Sprio, A Ruffini, G. Celotti, I. G. Lescib and N. Roveri, *J. Mater. Chem.*, 2009,**19**, 4973; (b) Y. P. Guo, L. H. Guo, Y. B. Yao, C. Q. Ning and Y. J. Guo, *Chem. Commun.*, 2011, **47**, 12215; (d) D. O. Costa, S. J. Dixon and A. S. Rizkalla, *ACS Appl. Mater. Interfaces*, 2012, **4**, 1490.

4 (a) H. H. Pan, X. Y. Liu, R. K Tang and H. Yao, *Chem. Commun.*, 2010,**46**, 7415; (b) L. J. Wang and G. H. Nancollas, *Chem. Rev.*, 2008, **108**, 4628; (c) J. W. Wang and L. L. Shaw, *Adv. Mater.*, 2007, **19**, 2364; (d) X. Y. Zhao, Y. J. Zhu, F. Chen, B. Q. Lu and J. Wu, *CrystEngComm*, 2013,**15**, 206; (e) K. L. Lin, X. G. Liu, J. Chang and Y. J. Zhu, *Nanoscale*, 2011, **3**, 3052.

5 (a) G. He, T. Dahl, A. Veis and A. Gorge, *Nat. Mater.*, 2003, **2**, 552; (b) R. K. Tang, M. Darragh, C. A. Orme, X. Y. Guan, J. R. Hoyer and G. H. Nancollas, *Angew. Chem. Int. Ed.*, 2005, **44**, 3698.

6 (a) B. Q. Xie and G. H. Nancollas, *PNAS*, 2010, **107**, 22369; (b) F. Nudelman, K. Pieterse, A. George, P. H. H. Bomans, H. Friedrich, L. J. Brylka, P. A. J. Hilbers, G. de With and N. A. J. M. Sommerdijk, *Nat. Mater.*, 2010, **9**, 1004; (c) A. George and A. Veis, *Chem. Rev.*, 2008, **108**, 4670.

7 (a) W. L. Murphy and D. J. Mooney, *J. Am. Chem. Soc.*, 2002, **124**, 1910; (b) X. Wang, J. Zhuang, Q. Peng and Y. D. Li, *Adv. Mater.*, 2006, **18**, 2031; (c) Y. Yuan, C. S. Liu, Y. Zhang and X. Q. Shan, *Mater. Chem. Phys.*, 2008, **112**, 275; (d) J. F. Hui, G. L. Xiang, X. X. Xu, J. Zhuang and X. Wang, *Inorg. Chem.*, 2009, **48**, 5614; (e) F. Chen, Y. J. Zhu, K. W. Wang and K. L. Zhao, *CrystEngComm*, 2011, **13**, 1858.

8 Y. Y. Hu, A. Rawal and K. Schmidt-Rohr, *PNAS*, 2010, **107**, 22425..

9 H. Ito, Y.Y. Oaki and H. Imai, *Cryst. Growth Des.*, 2008, **8**, 1055.

10 Y. H. Tseng, C. Y. Mou and J. C. C. Chan, *J. Am. Chem. Soc.*, 2006, **128**, 6909.

11 (a) E. S. Thian, Z. Ahmad, J. Huang, M. J. Edirisinghe, S. N. Jayasinghe, D. C. Ireland, R. A. Brooks, N. Rushton, W. Bonfield and S. M. Best, *Biomaterials*, 2008, **29**, 1833; (b) S. Boonrungsiman,

E. Gentleman, R. Carzaniga, N. D. Evans, D. W. McComb, A. E. Porter and M. M. Stevens, *PNAS*, 2012, **109**, 14170.
12 M. M. Stevens and J. H. George, *Science*, 2005, **310**, 1135.

Organoamine-assisted biomimetic synthesis of faceted hexagonal hydroxyapatite nanotubes with prominent stimulation activity for osteoblast proliferation

Xiangke Guo, Liang Yu, Lanhua Chen, Heyun Zhang, Luming Peng, Xuefeng Guo,* Weiping Ding

Received (in XXX, XXX) Xth XXXXXXXXX 200X, Accepted Xth XXXXXXXXX 200X
First published on the web Xth XXXXXXXXX 200X
DOI: 10.1039/b000000x

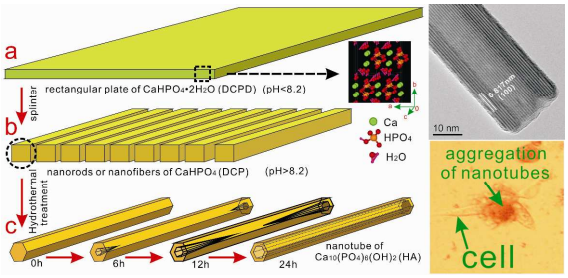

Uniform single-crystalline hydroxyapatite nanotubes were synthesized via a distinctive organoamines-assisted biomimetic route, and exhibited exceptional performance in stimulating osteoblast proliferation.